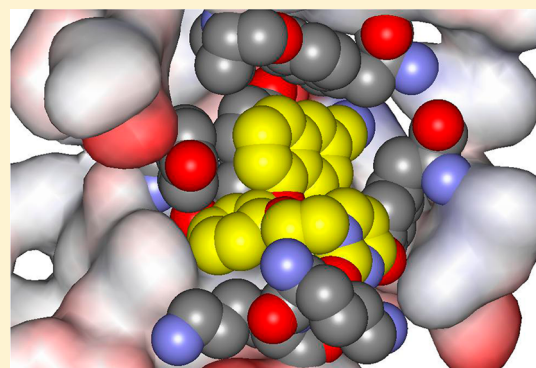


Picomolar Inhibitors of HIV-1 Reverse Transcriptase: Design and Crystallography of Naphthyl Phenyl Ethers

Won-Gil Lee,[†] Kathleen M. Frey,[‡] Ricardo Gallardo-Macias,[†] Krasimir A. Spasov,[‡] Mariela Bollini,[†] Karen S. Anderson,^{*,‡} and William L. Jorgensen^{*,†}[†]Department of Chemistry, Yale University, New Haven, Connecticut 06520-8107, United States[‡]Department of Pharmacology, Yale University School of Medicine, New Haven, Connecticut 06520-8066, United States

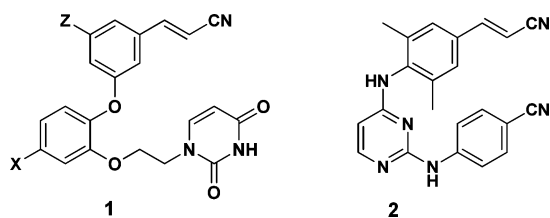
Supporting Information

ABSTRACT: Catechol diethers that incorporate a 6-cyano-1-naphthyl substituent have been explored as non-nucleoside inhibitors of HIV-1 reverse transcriptase (NNRTIs). Promising compounds are reported that show midpicomolar activity against the wild-type virus and sub-20 nM activity against viral variants bearing Tyr181Cys and Lys103Asn mutations in HIV-RT. An X-ray crystal structure at 2.49 Å resolution is also reported for the key compound **6e** with HIV-RT.



KEYWORDS: Anti-HIV agents, NNRTIs, protein crystallography

Non-nucleoside inhibitors of HIV-1 reverse transcriptase (NNRTIs) are a central component of anti-HIV chemotherapy.¹ In view of the continuing severity of the HIV/AIDS pandemic,² great effort is directed at seeking new compounds with improvements in activity toward variant strains of HIV-1 and in reducing dosages and undesirable side-effects.³ There are five FDA-approved NNRTIs including efavirenz and rilpivirine, which have particular importance since they are components of the one-a-day triple-combination therapies Atripla and Complera.¹ Our research has led to discovery of some extraordinarily potent NNRTIs in the catechol diether class.⁴ In particular, the dichloro (X, Z = Cl) and difluoro analogues of **1** have EC₅₀ values of 0.055 and 0.320 nM in an assay using human MT-2 cells infected with wild-type (WT) HIV-1, while efavirenz and rilpivirine have EC₅₀s of 2.0 and 0.670 nM.⁴



However, **1** like rilpivirine (**2**) bears a cyanovinylphenyl group, which may evoke concern as a potential Michael acceptor leading to off-target effects. In order to circumvent this, computational analyses led us to explore bicyclic replacements among which **3–5** provided very potent

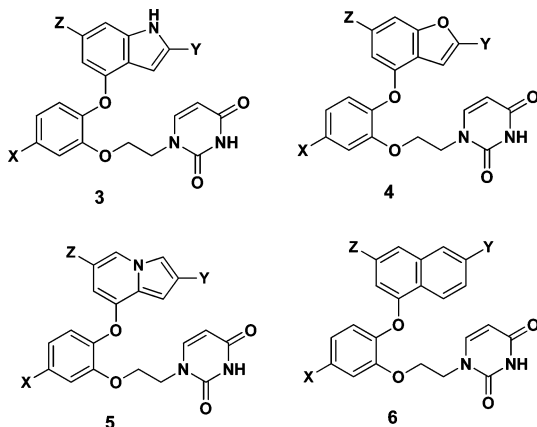
compounds.⁵ Other issues are also in play including activity toward viral variants containing clinically common mutations in HIV-RT, general cytotoxicity, and pharmacological properties, especially solubility. The two most commonly occurring mutations are Lys103Asn and Tyr181Cys.⁶ Indolizine **5a** (X = Z = H; Y = CN) is impressive in multiple regards; it has EC₅₀ values of 0.380 nM toward the WT virus and 11 nM toward HIV-1 bearing the challenging K103N/Y181C double mutation, it shows no cytotoxicity toward human T-cells (CC₅₀ > 100 μM), and it has good aqueous solubility, 38 μg/mL. By comparison, rilpivirine is somewhat less potent toward the WT virus (0.670 nM), somewhat more potent toward the double mutant (2.0 nM), significantly more cytotoxic (CC₅₀ = 8 μM), and far less soluble (ca. 0.1 μg/mL). However, oddly, in our assay with virus containing the single Y181C mutation, **5a** has an EC₅₀ of 310 nM, while rilpivirine yields 0.65 nM. Though we have also reported crystal structures of **5a** and four analogues of **1** and **2** with WT HIV-RT,^{5,7,8} clear explanation of the lower activity of **5a** toward the Y181C-bearing variant and the significant improvement toward the double mutant is elusive. For NNRTIs in general, it is almost always the case that activity is much reduced in going from the single to the double variant. Under the circumstances, we have continued to explore additional derivatives of the catechol diethers. Herein, the focus is on 1-naphthyl analogues **6**. These were not investigated

Received: September 10, 2014

Accepted: October 9, 2014

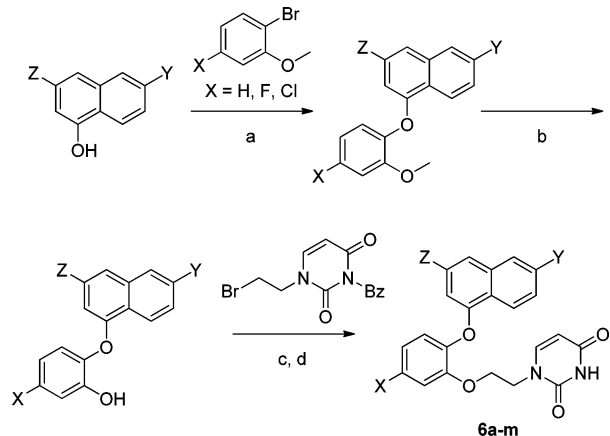
Published: October 13, 2014

earlier since it was unclear that their larger size would be accommodated in the NNRTI binding site and because among the variety of bicyclic heterocycles some could be expected to yield more optimal aryl–aryl interactions in the binding site.⁵



As summarized in Scheme 1, synthesis proceeded in a manner similar to that for 4 and 5.⁵ Substituted 1-hydroxynaphthalenes underwent Cu(I)-catalyzed addition to 2-bromoanisoles to yield naphthyl phenyl ethers. The methoxy group was unmasked with BBr_3 to give the phenols, which were alkylated with *N*-Bz-protected 1-bromoethyluracil and then deprotected. Full details are provided in the Supporting Information. The identity of assayed compounds was confirmed by ^1H and ^{13}C NMR and high-resolution mass spectrometry; HPLC analyses established purity as >95%. Aqueous solubilities were measured using a shake-flask procedure.^{5,9} Saturated solutions were made by stirring excesses of the compounds in Britton–Robinson buffer for 48 h at 25 °C. The pH of the buffer solutions is 6.5 as measured by a Corning General Purpose pH Combination probe (4136L21). The supernatant was collected using a Pall Life Sciences Acrodisc syringe filter with a 0.2 μm pore size and analyzed by UV–vis spectrophotometry (Agilent 8453). Piroxicam is used as a control; we consistently obtain values of 5–7 $\mu\text{g}/\text{mL}$, while the literature value is 5.9 $\mu\text{g}/\text{mL}$.⁹

Scheme 1. Synthesis of 1-Naphthyl Phenyl Ethers 6^a



^aReagents and conditions: (a) CuI, Cs_2CO_3 , 2,2,6,6-tetramethyl-3,5-heptanedione, dioxane, 100 °C, 48 h; (b) BBr_3 , DCM, –78 °C \rightarrow 0 °C, 3 h; (c) K_2CO_3 , DMF, 60 °C, 3 h; (d) NH_4OH , DCM, 16 h.

Table 1. Inhibitory Activity (EC_{50} , μM) for HIV-1 and Cytotoxicity (CC_{50} , μM) in MT-2 Cell Assays

compd	X	Y	Z	WT ^a	Y181C ^a	K103N/Y181C ^a	CC_{50} ^b
1a	Cl		Cl	0.00055	0.049	0.220	10
1b	F		F	0.00032	0.016	0.085	45
1c	H		Cl	0.00031	0.046	0.024	18
3a	H	CN	H	0.056	38	5.5	72
3b	H	CN	Me	0.010	NA	0.80	1.2
3c	H	CN	Cl	0.34	27	2.7	81
4a	H	CN	H	0.018	NA	0.42	>100
4b	H	CN	Cl	0.019	1.9	0.26	>100
4c	F	CN	H	0.040	3.5	4.0	>100
4d	Cl	CN	H	0.0070	NA	NA	7.0
5a	H	CN	H	0.00038	0.31	0.011	>100
5b	H	CN	Cl	0.0037	0.22	0.022	39
5c	H	CN	F	0.00070	0.17	0.068	40
5d	F	CN	H	0.0027	0.60	0.22	100
5e	F	CN	F	0.00040	0.25	0.010	50
5f	F	CN	Cl	0.0025	0.16	0.11	15
6a	H	H	H	0.060	5.7	5	80
6b	H	Me	H	0.25	12	15	40
6c	H	Cl	H	0.014	1.0	0.71	>100
6d	H	Cl	Cl	0.038	0.43	0.52	45
6e	H	CN	H	0.00053	0.019	0.015	>100
6f	H	CN	Cl	0.0022	0.013	0.0075	24
6g	F	CN	Cl	0.0045	0.0053	0.046	16
6h	Cl	CN	Cl	0.011	0.049	0.250	20
6i	F	CN	H	0.00049	0.010	0.048	>100
6j	Cl	CN	H	0.0015	0.048	0.150	>100
6k	H	CN	F	0.0011	0.008	0.006	>100
6l	F	CN	F	0.0019	0.0056	0.021	>100
6m	Cl	CN	F	0.005	0.032	0.150	18
nev ^c				0.11	NA	NA	>100
efv ^c				0.002	0.010	0.030	15
etv ^c				0.001	0.008	0.005	11
rpv ^c				0.00067	0.00065	0.002	8

^aFor 50% protection in MT-2 cells; NA for $\text{EC}_{50} > \text{CC}_{50}$ or >100 μM .
^bFor 50% inhibition of MT-2 cell growth. ^cNevirapine (nev); efavirenz (efv); etravirine (etv); and rilpivirine (rpv).

The procedures for the human MT-2 T-cell assays have been described in detail.^{4,5,10,11} Briefly, activities against the IIIB and variant strains of HIV-1 were measured; EC_{50} values are obtained as the dose required to achieve 50% protection of the infected MT-2 cells by the MTT colorimetric method. CC_{50} values for inhibition of MT-2 cell growth by 50% are obtained as well. The antiviral and toxicity curves used triplicate samples at each concentration.

The activity results for the naphthyl ethers are summarized in Table 1 along with corresponding data for key compounds in the 1 and 3–5 series and for four FDA-approved NNRTIs. This is the initial report for 1c and 6a–m. Among the naphthyl ethers, 6e, 6i, and 6k emerged as extremely potent NNRTIs. Before discussing the structure–activity data in more detail, it is helpful to present the crystallographic results for the complex of 6e with HIV-RT. As detailed in the Supporting Information, crystals were obtained using the recombinant RT52A enzyme that diffracted to 2.49 Å on the X29A beamline at the Brookhaven NSLS. A rendering of the NNRTI binding site from the structure is provided in Figure 1. Consistent with the crystal structures for 1a, 1b, and 5a,^{5,7} key interactions for 6e include aryl–aryl contacts with Tyr181, Tyr188, and Trp229

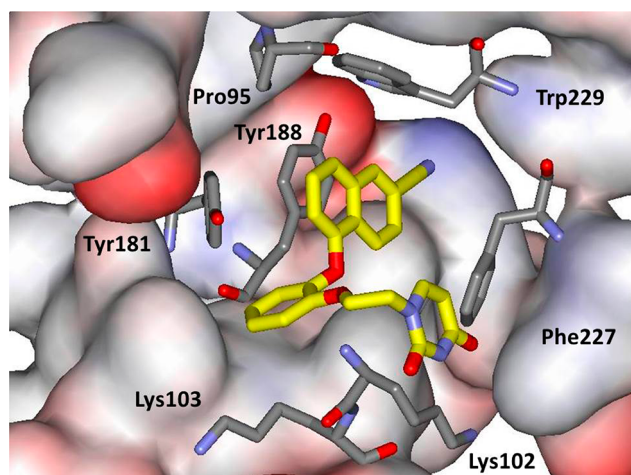


Figure 1. Rendering from the crystal structure of **6e** with wild-type HIV-1 reverse transcriptase. Carbon atoms of **6e** are colored yellow. Some residues in front of the ligand have been removed for clarity. The PDB code is 4WE1.

and the naphthyl fragment, a glancing edge-to-face interaction between Tyr181 and the catechol ring, and a hydrogen bond between the C2 carbonyl group of the uracil ring and the backbone NH of Lys103. The cyano group on C6 of the naphthalene projects into the channel leading to the RT polymerase active site; computer simulations using standard methods^{4,5} indicate that the cyano nitrogen is hydrogen-bonded to a water molecule.

The importance of the cyano group is apparent in the WT activities for **6a**, **6b**, **6c**, and **6e**; the unsubstituted **6a** is 100-fold less active than **6e**. The difference in the activities of the core structures is reflected in the data for **1c** (0.32 nM), **3c** (340), **4b** (19), **5b** (3.7), and **6f** (2.2), which are identically substituted with the cyano group and a chlorine. The activity for **1c** likely benefits from the added torsional degree of freedom for the cyanovinyl side chain, which allows some optimization of the interaction with Trp229. The torsion angle between the phenyl ring and vinyl group is 173° and 135° in the crystal structures for **1a** and **1b**,⁷ while in Monte Carlo simulations for the complex of **1a** and HIV-RT it ranges from 130–180° with an average of 155°.⁴ The naphthyl compound is then the next most active, followed by the indolizine. Among the cyanonaphthalenes, **6e–6m**, substitutions with fluorine or chlorine are not beneficial for WT activity except for the X = F analogue **6i**, which has similar potency to **6e** (0.5 nM). Additional options for substitution are limited owing to the tight packing in the binding site; aza analogues of the naphthalene group are also unlikely to be productive as there are no opportunities for hydrogen bonding with the aza nitrogens. In the indolizine series, the most potent compound is **5a**, the parent cyano analogue.

Turning to the results for the viral variants, significant gains have been made with the naphthyl ethers. There are multiple compounds with EC₅₀ values below 20 nM for the Y181C or K103N/Y181C variants. The reason for the more than 10-fold improvements toward the Y181C variant over the results for identically substituted indolizines appears to be subtle. When the crystal structures for **5a** and **6e** are overlaid, there is little difference except the indolizynyl fragment is tipped up toward Trp229 more than the naphthyl group. This causes the edge of the indolizine nearest Tyr181 (C6 and C7) to be a few tenths

Table 2. Experimental Aqueous Solubility at pH 6.5 (*S* in μg/mL) and Computed ClogP

cmpd	<i>S</i>	ClogP	cmpd	<i>S</i>	ClogP
1b	10.8	3.09	nev	167 ^a	2.65
1c	510	3.38	efv	68.0	4.67
5a	37.9	2.70	etv	<<1 ^b	5.22
5e	43.8	3.14	rpv	0.02 ^c	5.75
6e	4.3	3.30	rpv	0.24 ^d	5.75

^aReference 12. ^bReference 13. ^cReference 14; pH 7. ^dReference 15; pH 7.4.

of an angstrom closer to the tyrosine ring than for the left edge of the naphthalene ring system in Figure 1. Thus, the interaction between the indolizynyl fragment and Tyr181 may be more attractive than for naphthyl, and loss of the interactions in going to Cys181 is more damaging for **5** than **6**. Further crystallographic and computational analyses are being pursued.

The activity data for **6e**, **6f**, **6k**, and **6l** are particularly notable. Compounds **6k** and **6l** are more potent than efavirenz for all three viral strains, and **6k** is essentially identical to etravirine in potency. The naphthyl ethers are also less cytotoxic than efavirenz, etravirine, and rilpivirine with excellent results (CC₅₀ > 100 μM) for the very potent **6e**, **6i**, **6k**, and **6l**. The EC₅₀ results for etravirine and rilpivirine are impressive, though they are accompanied by extremely low solubility. The solubility data are summarized in Table 2, which includes previously unpublished results for **1c** and **6e**. As noted before, the normal range for solubility of oral drugs is 4–4000 μg/mL corresponding to an *S* of 10⁻²–10⁻⁵ M for a compound with a molecular weight of 400.^{16,17} Though **6e** barely makes it into this range, its solubility represents a ca. 40-fold improvement over etravirine and rilpivirine. The indolizines are an additional 10-fold more soluble, similar to efavirenz. For the cyanovinyl-phenyl series, a curious result is that, while the difluoro **1b** has a solubility of 11 μg/mL, duplicate measurements for the chloro analogue **1c** confirmed its remarkably high solubility, 510 μg/mL. The ClogP values for the listed catechol diethers are all near 3, which is again in the normal range of 0–5 for oral drugs,¹⁸ while etravirine and rilpivirine fall in the 5–6 region.

In summary, catechol diethers that incorporate a 6-cyano-1-naphthyl substituent have been explored as NNRTIs. Compounds **6e** and **6i** are very potent (0.5 nM) inhibitors of wild-type HIV-1, while **6k** has EC₅₀ values below 10 nM for all three viral strains. In comparison to heterobicyclic alternatives, the naphthyl ethers show improved performance against the variant strain of the virus incorporating the Tyr181Cys mutation in HIV-RT. Compound **6e** also shows much enhanced solubility in comparison to the most recently FDA-approved NNRTIs, etravirine and rilpivirine, though its solubility is 10-fold less than for the corresponding indolizine **5a**. A crystal structure for the complex of **6e** with WT HIV-RT confirmed the expected binding mode. Compounds such as **6e**, **6f**, and **6k**, which feature sub-20 nM potency toward all three viral strains and very low cytotoxicity, are promising for further study.

■ ASSOCIATED CONTENT

📄 Supporting Information

Synthetic procedures, NMR and HRMS spectral data for compounds **1c** and **6a–m**, and crystallographic details. The crystal structure data for the complex of **6e** and HIV-RT have

been deposited in the RCSB Protein Data Bank with the PDB code 4WE1. This material is available free of charge via the Internet at <http://pubs.acs.org>.

AUTHOR INFORMATION

Corresponding Authors

*(K.S.A.) E-mail: karen.anderson@yale.edu.

*(W.L.J.) E-mail: william.jorgensen@yale.edu.

Notes

The authors declare no competing financial interest.

ACKNOWLEDGMENTS

Gratitude is expressed to the National Institutes of Health (AI44616, GM32136, GM49551) for research support and for a fellowship to KMF (AI104334). We also thank the National Synchrotron Light Source at Brookhaven National Laboratory for beam time and assistance on X29A.

ABBREVIATIONS

HIV, human immunodeficiency virus; HIV-RT, HIV reverse transcriptase; NNRTI, non-nucleoside inhibitor of HIV-RT; Bz, benzoyl; DCM, dichloromethane; DMF, dimethylformamide; HPLC, high-performance liquid chromatography

REFERENCES

- (1) De Clercq, E. The Nucleoside Reverse Transcriptase Inhibitors, Nonnucleoside Reverse Transcriptase Inhibitors, and Protease Inhibitors in the Treatment of HIV Infections (AIDS). *Adv. Pharmacol.* **2013**, *67*, 317–358.
- (2) Reynolds, C.; de Koning, C. B.; Pelly, S. C.; van Otterlo, W. A. L.; Bode, M. L. In Search of a Treatment for HIV: Current Therapies and the Role of Non-Nucleoside Reverse Transcriptase Inhibitors (NNRTIs). *Chem. Soc. Rev.* **2012**, *41*, 4657–4670.
- (3) Zhan, P.; Chen, X.; Li, D.; Fang, Z.; De Clercq, E.; Liu, X. HIV-1 NNRTIs: Structural Diversity, Pharmacophore Similarity, and Implications for Drug Design. *Med. Res. Rev.* **2013**, *33*, E1–E72.
- (4) Bollini, M.; Domaoal, R. A.; Thakur, V. V.; Gallardo-Macias, R.; Spasov, K. A.; Anderson, K. S.; Jorgensen, W. L. Computationally-Guided Optimization of a Docking Hit to Yield Catechol Diethers as Potent Anti-HIV Agents. *J. Med. Chem.* **2011**, *54*, 8582–8591.
- (5) Lee, W.-G.; Gallardo-Macias, R.; Frey, K. M.; Spasov, K. A.; Bollini, M.; Anderson, K. S.; Jorgensen, W. L. Picomolar Inhibitors of HIV Reverse Transcriptase Featuring Bicyclic Replacement of a Cyanovinylphenyl Group. *J. Am. Chem. Soc.* **2013**, *135*, 16705–16713.
- (6) de Béthune, M.-P. Non-nucleoside Reverse Transcriptase Inhibitors (NNRTIs), Their Discovery, Development, and Use in the Treatment of HIV-1 Infection: A Review of the Last 20 Years (1989–2009). *Antiviral Res.* **2010**, *85*, 75–90.
- (7) Frey, K. M.; Bollini, M.; Mislak, A. C.; Cisneros, J. A.; Gallardo-Macias, R.; Jorgensen, W. L.; Anderson, K. S. Crystal Structures of HIV-1 Reverse Transcriptase with Picomolar Inhibitors Reveal Key Interactions for Drug Design. *J. Am. Chem. Soc.* **2012**, *134*, 19501–19503.
- (8) Frey, K. M.; Gray, W. T.; Spasov, K. A.; Bollini, M.; Gallardo-Macias, R.; Jorgensen, W. L.; Anderson, K. S. Structure-Based Evaluation of C5 Derivatives in the Catechol Diether Series Targeting HIV-1 Reverse Transcriptase. *Chem. Biol. Drug Des.* **2014**, *83*, 541–549.
- (9) Baka, E.; Comer, J. E. A.; Takács-Novák, K. Study of Equilibrium Solubility Measurement by Saturation Shake-Flask Method Using Hydrochlorothiazide as Model Compound. *J. Pharm. Biomed. Anal.* **2008**, *46*, 335–341.
- (10) Lin, T. S.; Luo, M. Z.; Liu, M. C.; Pai, S. B.; Dutschman, G. E.; Cheng, Y. C. Antiviral Activity of 2',3'-Dideoxy- β -L-5-fluorocytidine (β -L-EddC) and 2',3'-Dideoxy- β -L-cytidine (β -L-ddC) against Hep-

atitis B Virus and Human Immunodeficiency Virus Type 1 in Vitro. *Biochem. Pharmacol.* **1994**, *47*, 171–174.

(11) Ray, A. S.; Yang, Z.; Chu, C. K.; Anderson, K. S. Novel Use of a Guanosine Prodrug Approach to Convert 2',3'-Dideoxy-2',3'-dideoxyguanosine into a Viable Antiviral Agent. *Antimicrob. Agents Chemother.* **2002**, *46*, 887–891.

(12) Morelock, M. M.; Choi, L. L.; Bell, G. L.; Wright, J. L. Estimation and Correlation of Drug Water Solubility with Pharmacological Parameters Required for Biological Activity. *J. Pharm. Sci.* **1994**, *83*, 948–952.

(13) Weuts, I.; Van Dycke, F.; Voorspoels, J.; de Cort, S.; Stokbroekx, S.; Leemans, R.; Brewster, M. E.; Xu, D.; Segmuller, B.; Turner, Y. T. A.; Roberts, C. J.; Davies, M. C.; Qi, S.; Craig, D. Q. M.; Reading, M. Physicochemical Properties of the Amorphous Drug, Cast Films, and Spray Dried Powders to Predict Formulation Probability of Success for Solid Dispersions: Etravirine. *J. Pharm. Sci.* **2011**, *100*, 260–274.

(14) Janssen, P. A. J.; Lewi, P. J.; Arnold, E.; Daeyaert, F.; de Jonge, M.; Heeres, J.; Koymans, L.; Vinkers, M.; Guillemont, J.; Pasquier, E.; Kukla, M.; Ludovici, D.; Andries, K.; de Béthune, M.-P.; Pauwels, R.; Das, K.; Clark, A. D., Jr.; Frenkel, Y. V.; Hughes, S. H.; Medaer, B.; De Knaep, F.; Bohets, H.; De Clerck, F.; Lampo, A.; Williams, P.; Stoffels, P. In Search of a Novel Anti-HIV Drug: Multidisciplinary Coordination in the Discovery of 4-[[4-[[4-[(1E)-2-Cyanoethenyl]-2,6-dimethylphenyl]amino]-2-pyrimidinyl]amino]benzoxonitrile (R278474, Rilpivirine). *J. Med. Chem.* **2005**, *48*, 1901–1919.

(15) Sun, L.-Q.; Qin, B.; Huang, L.; Qian, K.; Chen, C.-H.; Lee, K.-H.; Xie, L. Optimization of 2,4-Diarylanilines As Non-Nucleoside HIV-1 Reverse Transcriptase Inhibitors. *Bioorg. Med. Chem. Lett.* **2012**, *22*, 2376–2379.

(16) Jorgensen, W. L.; Duffy, E. M. Prediction of Drug Solubility from Structure. *Adv. Drug Delivery Rev.* **2002**, *54*, 355–366.

(17) Bollini, M.; Cisneros, J. A.; Spasov, K. A.; Anderson, K. S.; Jorgensen, W. L. Optimization of Diarylazines As Anti-HIV Agents with Dramatically Enhanced Solubility. *Bioorg. Med. Chem. Lett.* **2013**, *23*, 5213–5216.

(18) Jorgensen, W. L. Efficient Drug Lead Discovery and Optimization. *Acc. Chem. Res.* **2009**, *42*, 724–733.